Competition between Rotamerization and Proton Transfer in *o*-Hydroxybenzaldehyde

Martin Čuma, Steve Scheiner,* and Tapas Kar

*Contribution from the Department of Chemistry, Southern Illinois University,
Carbondale, Illinois 62901-4409*

Received June 22, 1998. Revised Manuscript Received August 6, 1998

Abstract: The proton transfer from one oxygen atom to the other within the intramolecular H-bond in a molecule like *o*-hydroxybenzaldehyde (oHBA) would be precluded by a prior rotational isomerism that breaks this H-bond. The likelihood of such rotamerization in the ground and several excited electronic states is investigated by ab initio calculations at the CIS and MP2 levels with a 6-31+G** basis set. In the ground state, the energetics of proton transfer and rotamerization are competitive with one another; both processes are endothermic and must surmount an energy barrier. Excitation to the singlet or triplet $\pi\pi^*$ states presents a situation where tautomerization to the keto is exothermic, with a small barrier. In contrast, rotamerization is endothermic with high intervening barriers, so excited-state proton transfer is favored. The opposite situation is encountered in the nπ^* states, where rotations of the hydroxyl and carbonyl groups are facile and lead energetically downhill, in contrast to the high barriers opposing endothermic tautomerization. The computations provide insights into the fundamental causes for the discrepancies between the behaviors of the $\pi\pi^*$ and nπ^* states.

Introduction

Hydrogen bonds are present in a wide range of systems of chemical and biological importance. One dynamical process that a stereotypical AH···B H-bond may undergo is the transfer of the bridging hydrogen from group A to its partner B, forming A···HB. These proton-transfer reactions are integral to a myriad of processes, ranging from acid−base reactions to enzymatic catalysis. The importance and widespread occurrence of proton-transfer reactions has motivated an enormous amount of scrutiny from both experimental and theoretical perspectives.[1−9]

A model system that has generated a good deal of work over the years is *o*-hydroxybenzaldehyde (oHBA), also known as salicylaldehyde. As may be noted in Figure 1, this molecule contains an intramolecular H-bond between two oxygen atoms. There is some strain in this H-bond since the spatial restraints of the five-atom OCCCO system do not permit the bridging hydrogen to fit itself nicely along the O···O axis. This entire H-bonded ring system is squarely attached to an aromatic benzene ring. As such, oHBA is the prototype of a class of molecules that undergo proton transfer in a way that makes them particularly intriguing. The molecule is most stable in its so-called enol configuration, labeled **a** in Figure 1. A proton transfer to form the keto is energetically uphill. However, the situation reverses upon excitation to certain electronic states, such that the keto becomes favored over the enol. A photoexcitation can therefore directly induce a proton transfer to form the phototautomer. The relative energy reversal is also responsible for a large Stokes shift between the excitation and emission bands in this excited-state proton-transfer (ESPT) process. Moreover, the proton transfers from one tautomer to the other can take place very rapidly, on the picosecond (ps) or femtosecond (fs) time scale.

This particular combination of factors endows molecules of this sort with a wide range of potential applications such as design of new laser materials,[10−12] energy/data storage devices and optical switching,[13−15] Raman filters and hard-scintillation counters,[16] and polymer photostabilizers.[17,18] The ESPT process also has a number of biological applications, e.g. fluorescence probes,[19−21] and shows promise as a monitor of hydrophobic microenvironment, as in a micelle interior[22] and as a molecular probe for certain functional groups.[23]

---

* To whom correspondence should be addressed. E-mail: scheiner@chem.siu.edu.

(1) *Proton-Transfer Reactions*; Caldin, E., Gold, V., Eds.; Halsted Press: New York, 1975.

(2) Midland, M. M.; Morton, T. H. *J. Am. Chem. Soc.* **1993**, *115*, 9596.

(3) Planas, M.; Lee, C.; Novoa, J. J. *J. Phys. Chem.* **1996**, *100*, 16495.

(4) Florián, J.; Leszczynski, J. *J. Am. Chem. Soc.* **1996**, *118*, 3010.

(5) Tuckerman, M. E.; Marx, D.; Klein, M. L.; Parrinello, M. *Science* **1997**, *275*, 817.

(6) Bauer, S. H.; Wilcox, C. F. *Chem. Phys. Lett.* **1997**, *279*, 122.

(7) Sekikawa, T.; Kobayashi, T.; Inabe, T. *J. Phys. Chem. B* **1997**, *101*, 10645.

(8) Fernández-Ramos, A.; Rodríguez-Otero, J.; Ríos, M. A. *J. Phys. Chem. A* **1998**, *102*, 2954.

(9) Nishi, K.; Sekiya, H.; Kawakami, H.; Mori, A.; Nishimura, Y. *J. Chem. Phys.* **1998**, *109*, 1589.

(10) Chou, P.; McMorrow, D.; Aartsma, T. J.; Kasha, M. *J. Phys. Chem.* **1984**, *88*, 4596.

(11) Kasha, M. *Acta Physiol. Pol.* **1987**, *A71*, 717.

(12) Barbara, P. F.; Walsh, P. K.; Brus, L. E. *J. Phys. Chem.* **1989**, *93*, 29.

(13) Ferrer, M. L.; Acuña, A. U.; Amat-Guerri, F.; Costela, A.; Figuera, J. M.; Florido, F.; Sastre, R. *Appl. Opt.* **1994**, *33*, 2266.

(14) Douhal, A.; Sastre, R. *Chem. Phys. Lett.* **1994**, *219*, 91.

(15) Kuldová, K.; Corval, A.; Trommsdorff, H. P.; Lehn, J. M. *J. Phys. Chem. A* **1997**, *101*, 6850.

(16) Martinez, M. L.; Cooper, W. C.; Chou, P.-T. *Chem. Phys. Lett.* **1992**, *193*, 151.

(17) Heller, H. J.; Blattmann, H. R. *Pure Appl. Chem.* **1973**, *36*, 141.

(18) Werner, T.; Woessner, G.; Kramer, H. E. A. In *Photodegradation and Photostabilization of Coatings*; Pappas, S. P., Winslow, F. H., Eds.; American Chemical Society: Washington, DC, 1981; Vol. 151, p 1.

(19) Sytnik, A.; Kasha, M. *Proc. Nat. Acad. Sci. U.S.A.* **1994**, *91*, 8627.

(20) Sytnik, A.; Gormin, D.; Kasha, M. *Proc. Nat. Acad. Sci. U.S.A.* **1994**, *91*, 11968.

(21) Sytnik, A.; Litvinyuk, I. *Proc. Nat. Acad. Sci. U.S.A.* **1996**, *93*, 12959.

S0002-7863(98)02161-1 CCC: $15.00

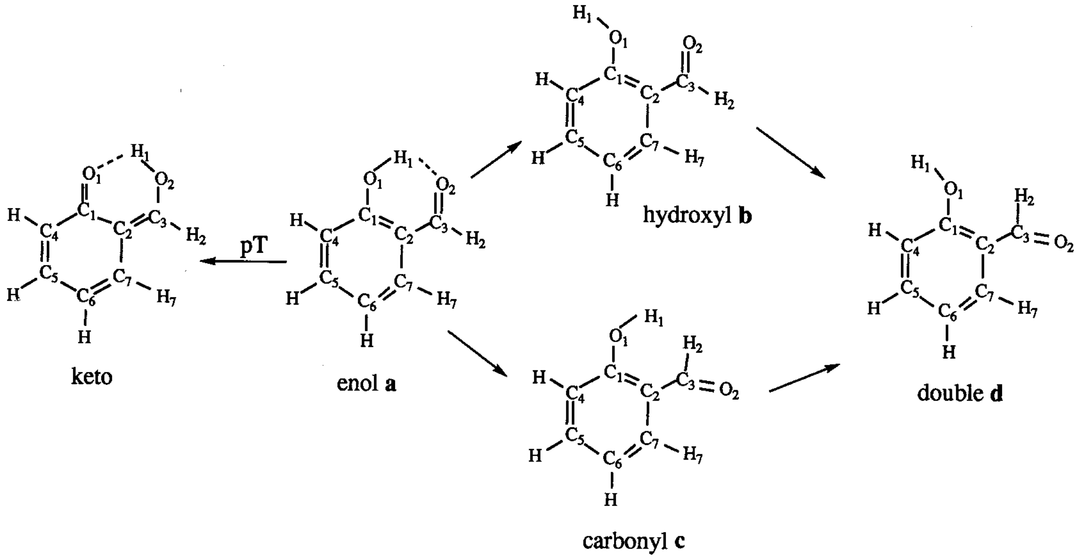

Figure 1. Structures of various rotamers of oHBA, including the atomic numbering scheme. Keto is formed from enol geometry **a** via a proton transfer. Rotamers **b**, **c**, and **d** result from rotations of hydroxyl and/or carbonyl groups.

The proton-transfer process in oHBA (and several closely related derivatives) in its ground and several low-lying excited states has been investigated by several groups.[24−29] The strained intramolecular H-bond in oHBA is expected to be rather weak, several kilocalories per mole at most. Consequently, it is reasonable to suppose that this bond can be broken by the rotation of either the hydroxyl or carbonyl group, leading to some of the rotamers in Figure 1. Indeed, there were a number of early suggestions that understanding of the spectra, and the underlying physics, requires not only knowledge about the proton-transfer itself but also information about the rotational isomerization that these molecules undergo.[30−33]

It is important to understand that the competitive energetics and dynamics of proton transfer versus rotational isomerism are important not only in the ground state but in the relevant excited states as well. That is, even if the molecule has been excited into an electronic state of the proper enol rotamer, a bond rotation in this excited state prior to the proton transfer will prevent the entire ESPT cycle from being completed successfully. A study of oHBA in a rare gas matrix[34] attempted to sort out the large number of possible rotamers that are possible within the context of a number of different excited states so as to interpret their spectral data, but with only limited success.

It is here that ab initio computations may make a significant contribution. A number of computations have in fact been performed on the proton-transfer process in oHBA,[29,35,36] but these works have not addressed the issue of bond rotations and how they might influence the entire process. The same is true of a recent paper from this laboratory which examined the energetics of the proton-transfer process in the ground and excited states of oHBA.[37] To derive a more comprehensive understanding of the entire process, we focus our attention here upon the various rotamerizations that this molecule can undergo, processes which might compete with the proton transfer. These isomerizations are studied in the ground and excited states and, in each case, compared to the possibility of a proton transfer in that same state.

Methods

Various conformers of the oHBA molecule are depicted in Figure 1. The enol form, designated rotamer **a**, contains a H-bond between the hydroxyl and carbonyl groups so is expected to be most stable. A rotation of the hydroxyl group by 180° breaks this bond, leaving the two oxygen atoms without a bridging proton in **b**; this configuration is referred to here as the hydroxyl rotamer. Rotation of the carbonyl group also breaks the H-bond and places two hydrogens near one another, as illustrated in **c**. Rotation of both groups yields the "double" rotamer **d**. The keto structure is obtained via proton transfer in the enol geometry, as opposed to any bond rotations.

The calculations were carried out at the ab initio level, using the Gaussian 94 package of codes.[38] The 6-31+G** basis set (five d functions)[39] was used to optimize the geometries which were performed at the SCF level for the ground states, and with CIS[40] for excited states. The effects of electron correlation upon the ground-state properties were examined by second-order Møller−Plesset perturbation theory (MP2).[41,42]

---

(22) Sarkar, N.; Das, K.; Das, S.; Datta, A.; Nath, D.; Bhattacharyya, K. *J. Phys. Chem.* **1995**, *99*, 17711.

(23) Douhal, A.; Dabrio, J.; Sastre, R. *J. Phys. Chem.* **1996**, *100*, 149.

(24) Gormin, D.; Heldt, J.; Kasha, M. *J. Phys. Chem.* **1990**, *94*, 1185.

(25) Douhal, A.; Lahmani, F.; Zehnacker-Rentien, A. *Chem. Phys.* **1993**, *178*, 493.

(26) Gai, F.; Fehr, M. J.; Petrich, J. W. *J. Phys. Chem.* **1994**, *98*, 8352.

(27) Lahmani, F.; Zehnacker-Rentien, A. *J. Phys. Chem. A* **1997**, *101*, 6141.

(28) Catalán, J.; Díaz, C. *J. Phys. Chem. A* **1998**, *102*, 323.

(29) Nagaoka, S.; Shinde, Y.; Mukai, K.; Nagashima, U. *J. Phys. Chem. A* **1997**, *101*, 3061.

(30) Acuña, A. U.; Amat-Guerri, F.; Catalán, J.; González-Tablas, F. *J. Phys. Chem.* **1980**, *84*, 629.

(31) Catalán, J.; Toribio, F.; Acuña, A. U. *J. Phys. Chem.* **1982**, *86*, 303.

(32) Toribio, F.; Catalán, J.; Amat, F.; Acuña, A. U. *J. Phys. Chem.* **1983**, *87*, 817.

(33) Bisht, P. B.; Petek, H.; Yoshihara, K.; Nagashima, U. *J. Chem. Phys.* **1995**, *103*, 5290.

(34) Morgan, M. A.; Orton, E.; Pimentel, G. C. *J. Phys. Chem.* **1990**, *94*, 7927.

(35) Nagaoka, S.; Nagashima, U. *Chem. Phys.* **1989**, *136*, 153.

(36) Sobolewski, A. L.; Domcke, W. *Chem. Phys.* **1994**, *184*, 115.

(37) Cuma, M.; Scheiner, S.; Kar, T. *Theochem*, in press.

(38) Frisch, M. J.; Trucks, G. W.; Schlegel, H. B.; Gill, P. M. W.; Johnson, B. G.; Robb, M. A.; Cheeseman, J. R.; Keith, T. A.; Petersson, G. A.; Montgomery, J. A.; Raghavachari, K.; Al-Laham, M. A.; Zakrzewski, V. G.; Ortiz, J. V.; Foresman, J. B.; Cioslowski, J.; Stefanov, B. B.; Nanayakkara, A.; Challacombe, M.; Peng, C. Y.; Ayala, P. Y.; Chen, W.; Wong, M. W.; Andres, J. L.; Replogle, E. S.; Gomperts, R.; Martin, R. L.; Fox, D. J.; Binkley, J. S.; Defrees, D. J.; Stewart, J. J. P.; Head-Gordon, M.; Gonzalez, G.; Pople, J. A. Gaussian, Inc., Pittsburgh, PA, 1995.

(39) Frisch, M. J.; Pople, J. A.; Binkley, J. S. *J. Chem. Phys.* **1984**, *80*, 3265.

(40) Foresman, J. B.; Head-Gordon, M.; Pople, J. A.; Frisch, M. J. *J. Phys. Chem.* **1992**, *96*, 135.

(41) Møller, C.; Plesset, M. S. *Phys. Rev.* **1934**, *46*, 618.

Table 1. Selected Bond Lengths (Å) and Angles (deg) of Various Conformers and Electronic States of oHBA[a]

	$O_1\cdots O_2$	O_1H_1	$O_2\cdots H_1$	O_1C_1	C_1C_2	C_2C_3	C_3O_2	C_3H_2	$H_2\cdots H_7$	$\theta(O_1H_1O_2)$
					enol **a**					
S_0	2.700	0.952	1.896	1.329	1.403	1.465	1.202	1.093	2.351	140.6
expt[b]	2.65	0.98		1.36	1.42	1.46	1.22	1.10		151
$^1n\pi^*$	0.102	−0.009	0.152	0.019	−0.004	0.009	0.055	−0.005	0.042	−4.8
$^3n\pi^*$	0.123	−0.011	0.180	0.022	−0.007	0.014	0.053	−0.009	0.051	−5.5
$^1\pi\pi^*$	−0.145	0.027	−0.227	−0.037	0.080	−0.041	0.035	−0.005	0.163	7.9
$^3\pi\pi^*$	0.025	−0.003	0.022	0.015	0.078	−0.025	0.016	−0.005	0.019	0.6
					hydroxyl **b**					
S_0	2.786	0.943		1.337	1.402	1.484	1.190	1.097	2.235	
$^1n\pi^*$	−0.131	0.000		0.013	−0.002	−0.021	0.067	−0.010	0.174	
$^3n\pi^*$	−0.143	0.000		0.017	−0.004	−0.018	0.068	−0.015	0.203	
$^1\pi\pi^*$	−0.023	0.003		−0.031	0.075	−0.038	0.019	−0.001	0.091	
$^3\pi\pi^*$	−0.013	0.000		0.008	0.082	−0.033	0.016	−0.005	0.044	

	$O_1\cdots H_2$	O_1H_1	$H_1\cdots H_2$	O_1C_1	C_1C_2	C_2C_3	C_3O_2	C_3H_2	$O_2\cdots H_7$
					carbonyl **c**				
S_0	2.649	0.941	1.945	1.347	1.396	1.478	1.193	1.096	2.492
$^1n\pi^*$	0.042	−0.001	0.023	0.007	0.004	−0.008	0.065	−0.011	0.058
$^3n\pi^*$	0.056	−0.001	0.035	0.009	0.001	−0.002	0.064	−0.015	0.068
$^1\pi\pi^*$	−0.029	0.004	−0.072	−0.035	0.074	−0.038	0.020	0.002	0.049
$^3\pi\pi^*$	0.009	−0.001	−0.002	0.011	0.052	−0.039	0.022	−0.007	−0.017
					double **d**				
S_0	2.425	0.943		1.349	1.395	1.484	1.195	1.089	2.520
$^1n\pi^*$	−0.049	0.000		0.005	0.008	−0.021	0.059	−0.002	0.111
$^3n\pi^*$	−0.037	0.000		0.008	0.005	−0.017	0.059	−0.006	0.123
$^1\pi\pi^*$	0.008	0.003		−0.034	0.073	−0.037	0.019	−0.001	0.028
$^3\pi\pi^*$	−0.007	0.001		0.005	0.073	−0.039	0.019	−0.005	−0.001

	$O_1\cdots O_2$	O_1H_1	$O_2\cdots H_1$	O_1C_1	C_1C_2	C_2C_3	C_3O_2	C_3H_2	$H_2\cdots H_7$	$\theta(O_1H_1O_2)$
					keto					
S_0	2.564	1.722	0.969	1.228	1.465	1.363	1.294	1.077	2.452	143.1
$^1n\pi^*$	0.181	0.294	−0.023	0.026	0.024	−0.017	0.042	−0.003	−0.043	−10.6
$^3n\pi^*$	0.230	0.356	−0.025	0.022	0.025	−0.022	0.047	−0.004	−0.054	−11.6
$^1\pi\pi^*$	0.054	0.067	−0.004	0.008	0.021	0.028	0.013	−0.002	0.011	−1.1
$^3\pi\pi^*$	0.138	0.203	−0.019	−0.013	0.021	0.000	0.028	−0.003	0.041	−5.2

[a] Excited-state parameters reported as difference, relative to S_0, of the same conformer. [b] Electron diffraction from ref 48.

As various means of incorporating electron correlation into ESPT provide inconsistent results,[43−45] no attempt has been made here to go beyond the CIS level for excited states. There is indeed some evidence that suggests CIS can provide useful treatment of certain excited states.[45−47]

The geometries of all four conformers were optimized, subject to the restriction that they are fully planar. This planarity was verified by 4-31G vibrational frequency computations which indicated no imaginary frequencies. The only exceptions were the excited states of the carbonyl rotamer **c**. Their imaginary frequencies involve out-of-plane motions that rotate the two hydrogens, H_1 and H_2, away from one another. Transition states for conversion from one rotamer to another were identified by again holding the molecule planar, with the exception of the group (hydroxyl or carbonyl) that is undergoing the rotation of interest.

Results

Geometries and Atomic Charges. The optimized geometries of the various conformers in their ground and excited electronic states are reported in Table 1. For each conformer, the optimized parameters are listed in the first row. The subsequent rows display the changes undergone by each parameter as a result of the excitation to the indicated electronic state.

Focusing attention first on the ground states, the calculated data for the enol in the first row of Table 1 are in reasonable coincidence with a gas-phase structure determined by electron diffraction[48] and reported in the succeeding row. The presence of an intramolecular H-bond in the enol rotamer **a** is supported by a comparison with the data for the hydroxyl rotamer **b**. The interoxygen distance is 2.70 Å in **a**, compared to 2.79 Å in **b**. (The value of 2.70 Å in **a** may be compared with the electron diffraction value of 2.65 Å.) Another indication of the H-bond is the 0.009 Å stretch in the O_1H_1 bond from 0.943 Å in **b** to 0.952 in **a**. This H-bond also affects the two C−O bonds. The O_1C_1 bond is shorter in **a** while C_3O_2 is longer, suggesting that the single bond of the former is strengthened and the double bond of the latter is weakened. The nominal C_2C_3 single bond is also particularly short in the H-bonded conformer **a**. Rotamer **c** of course contains no H-bond but has instead the possibility of H···H repulsion. The latter distance may be seen in the $H_1\cdots H_2$ (third) column of Table 1 to be 1.95 Å. In principle, one might envision an intramolecular H-bond between the hydroxyl oxygen O_1 and the carbonyl hydrogen H_2 in double rotamer **d**. However, these two atoms, separated by 2.425 Å, are probably too far apart to achieve a strong interaction. The same is true for the O_2 and H_7 atoms in **c** and **d**, which are separated by 2.49 and 2.52 Å, respectively.

---

(42) Pople, J. A.; Binkley, J. S.; Seeger, R. *Int. J. Quantum Chem., Quantum Chem. Symp.* **1976**, *10*, 1.

(43) Barone, V.; Adamo, C. *J. Chem. Phys.* **1996**, *105*, 11007.

(44) Sobolewski, A. L.; Sudholt, W.; Domcke, W. *J. Phys. Chem. A* **1998**, *102*, 2716.

(45) Paz, J. J.; Moreno, M.; Lluch, J. M. *J. Chem. Phys.* **1997**, *107*, 6275.

(46) Gittins, C. M.; Rohlfing, E. A.; Rohlfing, C. M. *J. Chem. Phys.* **1996**, *105*, 7323.

(47) Dickinson, J. A.; Hockridge, M. R.; Kroemer, R. T.; Robertson, E. G.; Simons, J. P.; McCombie, J.; Walker, M. *J. Am. Chem. Soc.* **1998**, *120*, 2622.

(48) Borisenko, K. B.; Bock, C. W.; Hargittai, I. *J. Phys. Chem.* **1996**, *100*, 7426.

Table 2. Natural Population Analysis[a] and Molecular Dipole Moment, μ

	O_1	O_2	H_1	H_2	C_1	C_2	C_3	sum	μ, D
enol **a**									
S_0	−0.772	−0.679	0.555	0.155	0.478	−0.324	0.530	−0.058	3.53
$^1n\pi^*$	−0.768	−0.252	0.526	0.269	0.377	−0.178	0.015	−0.009	2.06
$^3n\pi^*$	−0.770	−0.184	0.524	0.279	0.366	−0.159	−0.054	0.001	1.99
$^1\pi\pi^*$	−0.722	−0.761	0.579	0.167	0.544	−0.258	0.381	−0.070	4.62
$^3\pi\pi^*$	−0.781	−0.610	0.549	0.165	0.311	0.026	0.359	0.020	4.01
hydroxyl **b**									
S_0	−0.735	−0.607	0.512	0.135	0.456	−0.277	0.511	−0.005	4.66
$^1n\pi^*$	−0.761	−0.179	0.517	0.253	0.372	−0.153	0.005	0.052	2.03
$^3n\pi^*$	−0.767	−0.097	0.516	0.261	0.360	−0.132	−0.079	0.063	1.58
$^1\pi\pi^*$	−0.677	−0.666	0.524	0.138	0.544	−0.238	0.413	0.037	5.74
$^3\pi\pi^*$	−0.745	−0.545	0.512	0.148	0.332	0.023	0.363	0.087	4.31
carbonyl **c**									
S_0	−0.761	−0.628	0.517	0.124	0.441	−0.313	0.518	−0.102	2.28
$^1n\pi^*$	−0.776	−0.214	0.519	0.283	0.375	−0.152	0.016	0.051	0.52
$^3n\pi^*$	−0.766	−0.117	0.510	0.250	0.364	−0.159	−0.078	0.004	0.87
$^1\pi\pi^*$	−0.714	−0.692	0.538	0.116	0.546	−0.265	0.385	−0.086	4.59
$^3\pi\pi^*$	−0.770	−0.555	0.515	0.142	0.287	0.003	0.334	−0.045	2.03
double **d**									
S_0	−0.767	−0.639	0.519	0.166	0.433	−0.281	0.516	−0.052	5.14
$^1n\pi^*$	−0.764	−0.195	0.511	0.241	0.376	−0.179	0.002	−0.008	2.71
$^3n\pi^*$	−0.777	−0.141	0.519	0.292	0.364	−0.131	−0.063	0.063	2.27
$^1\pi\pi^*$	−0.714	−0.685	0.531	0.162	0.544	−0.212	0.396	0.022	7.06
$^3\pi\pi^*$	−0.775	−0.575	0.520	0.181	0.315	0.032	0.352	0.050	4.78

[a] SCF values listed for the ground state and CIS for excited states.

The changes in the $R(O_1 \cdots O_2)$ distance caused by electronic excitation provide particularly clear evidence of the H-bond perturbations. This distance is stretched by 0.1 Å in the two $n\pi^*$ states, which suggests a substantial weakening of the H-bond. This supposition of H-bond weakening is reinforced by the 0.01 Å contraction in the O_1H_1 bond, as well as the reduction in the $\theta(O_1H_1O_2)$ angle further from its ideal value of 180°. The strengthening of the H-bond that is associated with the $^1\pi\pi^*$ state is clearly visible in the contraction of $O_1 \cdots O_2$, a much longer O_1H_1, and an 8° straightening of $\theta(O_1H_1O_2)$.

A glance at the structure of the carbonyl rotamer **c** might lead to the expectation of a repulsion between the H_1 and H_2 atoms. However, they are nearly 2 Å apart so this repulsion is likely to be fairly small. Moreover, the $H_1 \cdots H_2$ distance is little affected by electronic excitation, the major exception being a reduction of this separation by 0.07 Å in the $^1\pi\pi^*$ state. The $n\pi^*$ excitations produce a 0.04−0.05-Å reduction in the distance separating O_1 and H_2 in the double rotamer **d**, which might be associated with an enhanced interaction and a possible H-bond. However, the latter idea is belied by the absence of any noticeable change in the O_1H_1 bond length.

One last curious pattern is related to the $^1\pi\pi^*$ state. Regardless of which conformer is being considered (exclusive of keto), excitation to the latter electronic state yields almost the same pattern of change on several of the bonds. This excitation shortens the O_1C_1 bond by about 0.03, stretches C_1C_2 by 0.07 Å, shortens C_2C_3 by 0.04 Å, and finally elongates C_3O_2 by 0.02−0.03 Å. The triplet also shows some regularity from conformer to conformer but not to the same degree as $^1\pi\pi^*$.

The natural population charges displayed in Table 2 provide some clues regarding some of the geometry changes of the various conformers. In comparison to the other three rotamers in their ground states, enol **a** has the most negative O_1 and O_2 atoms, along with the most positive H_1, all features characteristic of a H-bond between the two oxygens. The most positive charge for H_2 occurs in the double conformer **d**. This finding, along with the enhanced negative charge on O_1, supports the idea of a H-bond here, albeit a weak one. An alternative viewpoint which ignores the H-bond possibility would ascribe any attraction between O_1 and H_2 to purely electrostatic phenomena.

The most dramatic effects of electronic excitation are exhibited by the O_2 atom which has a charge of around −0.6 in each ground state. $n \rightarrow \pi^*$ excitation lowers this negative charge a great deal for each conformer; it is affected much less by $\pi \rightarrow \pi^*$ excitation, and one can observe a clear tendency for the $^1\pi\pi^*$ state to enhance this atom's negative charge. The much smaller negative charge of O_2 in the $n\pi^*$ states can be ascribed to the displacement of an electron out of the n MO, which is largely a lone pair on this atom. The weakening of the H-bond in conformer **a** is responsible for the $O_1 \cdots O_2$ lengthening. Likewise, the reduced negative charge on O_2 lessens the electrostatic repulsion with O_1 in hydroxyl rotamer **b**, accounting for the contraction of $O \cdots O$ in the $n\pi^*$ excited states. One can also understand the closer approach of the O_1 and H_2 atoms in the $n\pi^*$ states of double rotamer **d** in terms of the enhancement of the positive charge on the latter as a result of this excitation.

It should be noted that the trends described here for the natural charges are not particular to this method of charge assignment. Mulliken populations reveal very similar patterns, although the absolute Mulliken charges of course differ from the natural charges.

The dipole moment computed for each rotamer is reported in the last column of Table 2. The moment of the enol structure in its ground state is 3.53 D. Rotation of the hydroxyl group increases this quantity to 4.66 D, whereas a decrease results from the rotation of the carbonyl group. The highest moment of all is associated with the double rotamer **d**. Since the various rotamers are all planar, the moment lies in the molecular plane in each case. Each rotamerization carries with it also a change in the moment's direction, in each case consistent with the specific motions of the atoms, and their atomic charges listed in Table 2. For each rotamer, $n \rightarrow \pi^*$ excitation reduces the moment's magnitude. This reduction is consonant with the displacement of an electron from the molecular plane to the π

Table 3. Adiabatic Excitation Energies (kcal/mol)

conformer	$^1n\pi^*$	$^3n\pi^*$	$^1\pi\pi^*$	$^3\pi\pi^*$
enol **a**	116.8	101.4	118.1	73.6
hydroxyl **b**	107.2	90.6	125.2	71.9
carbonyl **c**	110.0	94.4	121.7	71.2
double **d**	108.6	92.1	124.2	69.0
double **d** (expt)[a]	75.4	70.7	90.9	
keto	117.3	105.5	95.4	43.4

[a] From ref 34.

Table 4. Energies (kcal/mol) of the Various Rotamers Compared to Enol **a** in the Same Electronic State

	S$_0$		$^1n\pi^*$	$^3n\pi^*$	$^1\pi\pi^*$	$^3\pi\pi^*$
	SCF	MP2	CIS	CIS	CIS	CIS
enol **a**	0.0	0.0	0.0	0.0	0.0	0.0
hydroxyl **b**	9.7	10.3	0.2	−1.1	16.8	7.9
carbonyl **c**	8.8	7.7	2.1	1.3	12.4	5.9
double **d**	5.9	7.1	−2.3	−3.0	12.0	1.7
keto	16.1	16.5	16.6	20.2	−6.7	−14.2

system, taking into account also that the n orbital consists largely of an oxygen lone pair. The $\pi\rightarrow\pi^*$ excitations generally have a less dramatic effect on the dipole moment, probably because neither of these orbitals lies in the molecular plane, wherein lies the moment. It is intriguing to note that the $^1\pi\pi^*$ moment is in all cases larger than that of the triplet, and in some cases by quite a significant amount.

Energetics. The energies required to excite each conformer to the indicated excited state are reported in Table 3. These values refer to adiabatic excitations in which the excited state is free to relax to its optimized geometry upon completion of the excitation. In accord with our earlier findings, the $^3\pi\pi^*$ state of the enol is lowest in energy, followed in order by $^3n\pi^*$, then the two singlets which are rather close in energy to one another, but with $^1n\pi^*$ being slightly preferred. This pattern is repeated for the other conformers with the exception that the $^1n\pi^*$ state is much more clearly lower in energy than is $^1\pi\pi^*$. The various bond rotations that yield conformers **b**, **c**, and **d** produce several changes in excitation energy. Whereas the $^3\pi\pi^*$ state is little affected, the two $n\pi^*$ states drop by 7−11 kcal/mol and $^1\pi\pi^*$ rises by 4−7 kcal/mol.

An additional conformer is listed in the final row of Table 3. The keto is similar to the enol, except that the H_1 proton has transferred across from O_1 to O_2 (the keto is commonly referred to as the tautomer of the enol). This proton transfer produces large changes in the excitation energies of the $\pi\pi^*$ states. The $^3\pi\pi^*$ excitation energy drops by 30 kcal/mol, and the singlet $^1\pi\pi^*$, by more than 20 kcal/mol. The excitation energies of the two $n\pi^*$ states are relatively unaffected remaining stable to within 4 kcal/mol. These large changes in the $\pi\pi^*$ states alter the ordering of states. In the case of the keto tautomer, the $^3\pi\pi^*$ state remains lowest in energy but the singlet $^1\pi\pi^*$ drops from highest in energy to second lowest.

A previous measurement[34] of the excitation energies of several of these states in the double rotamer **d** yielded values smaller than our calculated results. As reported in Table 3, the calculated data are overestimated by some 20−30 kcal/mol. In fact, CIS is known to yield poor quantitative excitation energies so this result is not surprising.[36,49,50] What is most encouraging is that the error is fairly uniform and that the CIS excitations follow the same ordering of states as observed experimentally. Indeed, the calculated difference between the two singlet states, 15.6 kcal/mol, is in remarkably good coincidence with the experimental difference of 15.5 kcal/mol.

An alternate means of comparing energies is presented in Table 4. For each electronic state, the energy of each conformer is indicated relative to that of the enol **a**. For example, at the SCF level, the enol is clearly the lowest in energy of the various conformers in the ground state. The double rotamer **d** is 6 kcal/mol higher in energy, followed in order by the carbonyl and hydroxyl rotamers. The keto tautomer is considerably higher in energy than any of the other rotamers. Incorporating electron correlation into the ground state via MP2 changes the quantitative results only a small amount, and the qualitative conclusions, not at all.

Turning now to the excited states, there is a clear division between the two $n\pi^*$ states on one hand and the $\pi\pi^*$ states on the other. For the $n\pi^*$ states, the keto tautomer remains higher in energy than the enol by some 16−20 kcal/mol. However, the rotamers are lowered to the point where they are at least comparable to the enol. Note for example that the double rotamer **d** is predicted to be 2−3 kcal/mol lower in energy than the enol in these states.

The situation is quite different for the $\pi\pi^*$ states where the keto is the lowest energy structure, and by a significant margin. The various other conformers, even **d**, are clearly higher in energy than the enol. For the $^1\pi\pi^*$ state in particular, the three rotamers **b**, **c**, and **d** are all 12−17 kcal/mol higher in energy than the enol, and even more disfavored when compared to the keto. In contrast, the triplet $\pi\pi^*$ state favors the rotamers somewhat more, with relative energies slightly lower than in the ground state. Most notable of all, however, is the strong preference for the keto tautomer in the $^3\pi\pi^*$ state, amounting to a 30 kcal/mol reversal of the situation in the ground state. (The underlying cause of this keto stabilization was discussed in our earlier paper.[37])

Some of these energy patterns are consistent with the geometric and charge trends displayed in Tables 1 and 2. Consider, for example, the $n \rightarrow \pi$ excitation, either singlet or triplet. There was clear geometric evidence that this excitation weakened the intramolecular H-bond in the enol, while simultaneously reducing any $O_1 \cdots O_2$ repulsion in the hydroxyl rotamer **b**. Both of these observations were reinforced by the excitation-induced precipitous drop of negative charge on the O_2 atom. Likewise, this same excitation shows evidence of strengthening the interaction between O_1 and H_2 in the double rotamer **d**: the interatomic distance drops and their opposite charges both increase in magnitude. The enhanced stability of the enol, relative to the three rotamers, in the $^1\pi\pi^*$ state, is attributable in part to the strengthening of the intramolecular H-bond in the enol.

The relative energies listed in Table 4 say little about the likelihood of transitions from one rotamer to another. For that purpose, one must also have at hand information about the energy barriers separating the various conformers. These barriers were computed by locating the transition states,[51] and the data are reported in Table 5. Beginning with the ground state, transitions from the enol are all rather high in energy. Rotations from **a** to either the **b** or **c** rotamers are all impeded by a barrier of at least 13 kcal/mol. As indicated by the last row of Table 5, the proton transfer to the keto must also

---

(49) Luth, K.; Scheiner, S. *J. Phys. Chem.* **1994**, *98*, 3582.

(50) Luth, K.; Scheiner, S. *J. Phys. Chem.* **1995**, *99*, 7352.

(51) The rotation of atoms out of the molecular plane causes a loss of the strict separation between σ and π orbitals. This problem is minimal for hydroxyl rotation since motion of the hydrogen causes minor disruptions. Rotation of the carbonyl group, on the other hand, causes motion of an oxygen as well as hydrogen out of the plane. For that reason, some caution should be exercised in interpretation of the $\pi\pi^*$ barriers of the excited states.

Table 5. Rotational and Proton Transfer Barriers (kcal/mol)

		S_0		$^1n\pi^*$	$^3n\pi^*$	$^1\pi\pi^*$	$^3\pi\pi^*$
	type	SCF	MP2	CIS	CIS	CIS	CIS
a → **b**	rot	13.0	13.8	1.5	0.2	24.0	9.6
a → **c**	rot	16.0	15.0	2.2	*a*	32.7	16.2
b → **d**	rot	5.0	3.7	4.8	3.5	14.0	7.7
c → **d**	rot	0.8	2.9	*a*	*a*	7.8	*a*
a → keto	pT	18.0	12.6	30.2	36.6	2.8	6.8

[a] No barrier encountered.

surmount a high barrier. These conclusions are not altered substantially by inclusion of electron correlation.

The situation is rather different in the excited states. In the case of the $n\pi^*$ states, the proton transfer to the keto is made very difficult by an even higher barrier, in excess of 30 kcal/mol. In contrast, rotation of either the hydroxyl or carbonyl group is rather facile, with barriers of 2 kcal/mol or less. Indeed, in the case of the $n\pi^*$ states, there is no barrier at all for rotation of the carbonyl group. Upon reaching either rotamer **b** or **c**, a second rotation of the other group to form the most stable rotamer **d**, is opposed by small barriers as well. In effect then, the rotations of the hydroxyl and carbonyl groups are nearly free, while proton transfer faces a very high barrier.

The $\pi\pi^*$ states present a nearly opposite situation. As mentioned above, the rotamers are all higher in energy than the enol, particularly for $^1\pi\pi^*$. The barriers which must be surmounted to reach these rotamers are even higher. For example, the lowest barrier facing enol **a** is 9.6 kcal/mol in the $^3\pi\pi^*$ state for rotation of the hydroxyl group. Rotational barriers in the $^1\pi\pi^*$ state are both over 20 kcal/mol. In contrast to these high barriers opposing rotations, the proton-transfer barriers are much lower in the two $\pi\pi^*$ states, 7 kcal/mol or less.

The competition between rotational motions and proton transfer, and their connections with excitation energies, can be readily visualized in Figure 2, which places intermediates and transition states on a common energy scale. The proton transfer involved in enol → keto tautomerization is illustrated to the left of the enol, while the rotations are exhibited to its right. The overall comparable barriers to proton transfer and rotation of the ground state are clear from the lowest part of the figure. The first excited state is the $^3\pi\pi^*$ state, and it can clearly undergo a proton transfer more readily than the rotations involved in reaching the double rotamer **d**. This is even more correct for the $^1\pi\pi^*$ state, so much so that the $^1\pi\pi^*$ rotamers are the highest energy structures in Figure 2. The ease with which the $n\pi^*$ state can undergo rotation, as compared to their high proton-transfer barriers, is also apparent in Figure 2.

The specific rotation pathway illustrated in Figure 2 is **a** → **b** → **d**, which corresponds to rotation of the hydroxyl group, followed by the carbonyl. The alternate stepwise path would reverse this order, i.e., **a** → **c** → **d**. While not shown explicitly in Figure 2, the aforementioned conclusions hold for this pathway as well. Specifically, proton transfer in the $\pi\pi^*$ states is preferred to **a** → **c** → **d** rotations, whereas the $n\pi^*$ states are characterized by a much more facile pair of rotations as compared to proton transfer. In terms of which pathway would be more favorable to rotamerization in the $n\pi^*$ states, there might be a small preference for **a** → **b** → **d**.

Discussion and Conclusions

There have been earlier computations of the four rotamers with which some of our results may be compared, although these earlier works were limited to the ground state. Not surprisingly, SCF/6-31G** calculations[52] predicted relative energies very similar to our own 6-31+G** data in the first column of Table 4. A much smaller minimal basis set was found to be capable of reproducing the correct ordering of the four rotamers, although the energies were quantitatively skewed. A more recent set of calculations[53] addressed the same question of rotamer relative energies, again in their ground states. These data again agreed nicely with our computations in Table 4 and further demonstrated a lack of sensitivity to details of the basis set, such as the presence or absence of diffuse functions or the number of valence or polarization functions. This insensitivity applies not only to energetics but to geometrical parameters as well. The application of density functional theory (DFT) raised the relative energies by several kilocalories per mole. This increase is consistent with the incorporation of electron correlation into DFT and the increases observed here by using MP2.

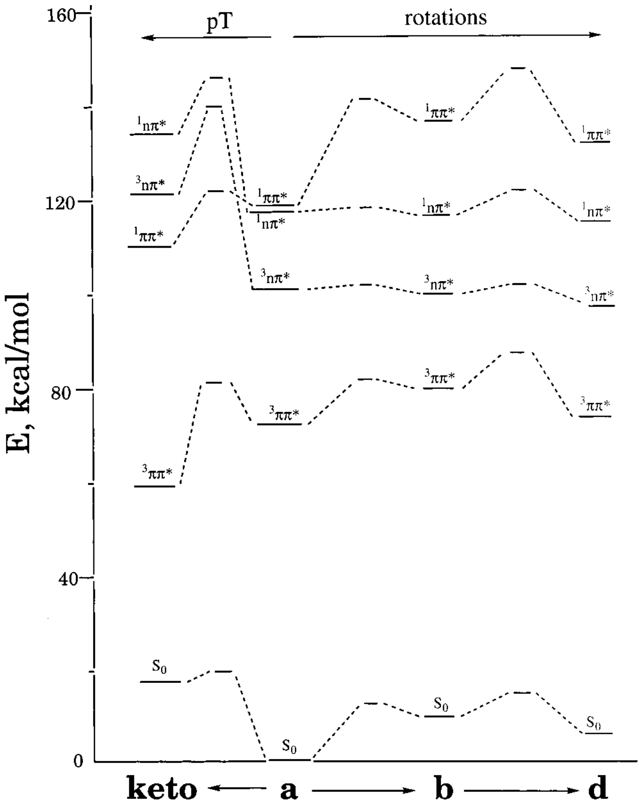

Figure 2. Energies computed for various conformers in several electronic states. Levels between minima correspond to transition states. The **a** → **b** → **d** rotation pathway shown corresponds to rotation of carbonyl followed by hydroxyl. The alternate **a** → **c** → **d** pathway exhibits similar energetics.

There are experimental estimates of some of these relative energies, but these data are not entirely consistent. Early ultrasonic relaxation data[54] suggested that there is a second conformer in addition to the enol in the ground state, perhaps 2.3 kcal/mol higher in energy, but the authors were unable to identify its character. Later IR spectral measurements[55] indicated that this second conformer may correspond to double rotamer **d** but was certainly less than definitive; the energy difference was estimated to be 2.8 kcal/mol.

---

(52) Schaefer, T.; Sebastian, R.; McKinnon, D. M.; Spevack, P. W.; Cox, K. J.; Takeuchi, C. S. *Can. J. Chem.* **1993**, *71*, 960.

(53) Chung, G.; Kwon, O.; Kwon, Y. *J. Phys. Chem. A* **1998**, *102*, 2381.

(54) Rajagopal, E.; Sivakumar, K. V.; Subrahmanyam, S. V. *J. Chem. Soc., Faraday Trans. 1* **1981**, *77*, 2149.

(55) Radhi, M. M.; El-Bermani, M. F. *Spectrochim. Acta* **1990**, *46A*, 33.

The most comprehensive data emerge from IR spectra in rare gas matrices.[34] After irradiation with a 325-nm laser to the $^1n\pi^*$ excited state, double rotamer **d** appears. This result is consistent with our finding that this conformer is the most stable one in the $n\pi^*$ manifold. Moreover, the identification by Morgan et al. that the S_1 and S_2 states of **d** correspond to $^1n\pi^*$ and $^1\pi\pi^*$, respectively, agrees with our computations. In terms of relative energies, by combining their data with earlier experimental estimates of ground-state energetics, Morgan et al. concluded that double rotamer **d** is close in energy to the enol in the $^1n\pi^*$ state. Their result differs with ours in that they estimate **a** to be more stable by 2.7 kcal/mol, while our calculations predict **d** is favored by 2.3. Experiment and calculations converge nicely for the $^1\pi\pi^*$ state, where both predict **a** to be lower in energy, experiment by 13.7 kcal/mol, theory by 12.0.

Morgan[34] et al. were also able to delve into rotational barriers to a certain extent. The rotamerization from **a** to **d** was proposed to involve an intervening energy barrier in the two excited singlets. Note first that the experimental estimate did not attempt to differentiate a direct **a** → **d** path, i.e., a simultaneous double rotation, from a stepwise pathway, **a** → **b,c** followed by **b,c** → **d**, as in our calculations. Nonetheless, it is instructive to compare the results. The experimental estimate for the $^1n\pi^*$ barrier of 8.4 kcal/mol is somewhat higher than our computed **b** → **d** barrier of 4.8. The experimental 17.7 kcal/mol barrier for the $^1\pi\pi^*$ state is in the same range as, but perhaps smaller than, the calculated barriers listed in Table 5. An electron diffraction estimate of the barrier to rotation of the carbonyl group, in the ground state, is some 7.2 kcal/mol[48] smaller than our SCF and MP2 values of 15−16.

The experimental verification that double rotamer **d** is likely more stable than **b** and **c**, in which only one group has been rotated, motivated us to investigate whether the simultaneous double rotation might in fact be more facile than the stepwise process. Examination of the potential energy surface provided evidence that a simultaneous pair of rotations would encounter an energy barrier comparable to those along the single-transfer pathways. The optimal pathway would thus skirt around the maximum in the surface along the synchronous rotation. This result suggests that while there may be a certain degree of concertedness in the rotations, the process would better be categorized as stepwise than as simultaneous.

Some of the disagreement between experiment and theory may be due to the suggestion by Morgan et al. that they might in fact be observing reactions in vibrationally excited levels or that the triplet surface may be involved in what they analyze as purely singlet. Indeed, there is computational confirmation of the latter supposition. With little hard data to guide them, the authors guessed that the triplet surface might be a repulsive one, leading directly from **a** to **d**. Indeed a glance at the $^3n\pi^*$ profile in Figure 2 reveals a strong possibility that their guess was correct, as there are indeed very low barriers along the **a** → **b** → **d** pathway which is energetically downhill. This observation adds further credence to the notion that the observed difference in reaction quantum yields is due to a low-barrier triplet forward reaction that dominates over the ground-state reverse process which the calculations predict to contain high barriers.

Our calculations lead to the following conclusions with respect to the energetics of oHBA. The proton transfer leading from enol to keto is energetically uphill for the ground and $n\pi^*$ states. In contrast, the keto is favored for the two $\pi\pi^*$ states. The barrier to transfer in the latter states is fairly low, particularly for the singlet. Consequently, a photoinduced proton transfer would be facile in the $\pi\pi^*$ states and unlikely in the others. With respect to bond rotations, the enol conformer is most stable in the ground state. In contrast, structure **d** which involves the 180° rotation of both the hydroxyl and carbonyl groups, would appear to be favored in the $n\pi^*$ states. The other rotamers, corresponding to rotations of only one group or the other are also fairly low in energy. This observation, coupled with the low barriers computed to bond rotation, makes rotamerization a likely process in the $n\pi^*$ states. These bond rotations are certainly favored over proton transfer which is energetically uphill and involves a high barrier. The opposite situation is encountered in the $\pi\pi^*$ states where the proton transfer is favored by a low barrier to an exothermic process. Bond rotations are unlikely since the rotamers are considerably higher in energy than the enol structure and generally are associated with high barriers. A possible exception is the double rotamer **d** of the $^3\pi\pi^*$ state which may be competitive in energy with the enol. Nonetheless, there would appear to be a high barrier separating **d** from the enol, which would mitigate against this rotamerization, thereby favoring the proton transfer.

In summary, then, excitation to either of the $\pi\pi^*$ states would be conducive to the ESPT process as the enol → keto proton transfer would be favored over any earlier rotamerization that would preclude the transfer in these excited states. In contrast, if excited to a $n\pi^*$ state, the oHBA molecule would likely undergo a rapid rotamerization to a structure like **d** which cannot undergo an intramolecular proton transfer.

Acknowledgment. This work was supported by a grant from the National Science Foundation (CHE-9123824). M.Č. is grateful to SIU for a Dissertation Research Award.

JA982161X